Title

Porous Polymers as Universal Reversal Agents for Heparin Anticoagulants through an Inclusion—Sequestration Mechanism

Journal

Advanced Materials, 34(23)

ISSN

0935-9648

Authors

Lin, Furong

Yu, Shang-Bo

Liu, Yue-Yang

et al.

Publication Date

2022-06-01

DOI

10.1002/adma.202200549

Porous polymers as universal reversal agents for heparin anticoagulants through an adsorption-sequestration mechanism

Furong Lin[1], Shang-Bo Yu[1]*, Yue-Yang Liu[2], Chuan-Zhi Liu[2], Shuai Lu[3], Jin Cao[1], Qiao-Yan Qi[1], Wei Zhou[2]*, Xiaopeng Li[3], Yi Liu[4], Jia Tian[1] and Zhan-Ting Li[1,2]*

[1]Key Laboratory of Synthetic and Self-Assembly Chemistry for Organic Functional Molecules, Shanghai Institute of Organic Chemistry, Chinese Academy of Sciences, 345 Lingling road, Shanghai 200032, China

[2]Department of Chemistry, Fudan University, 2205 Songhu Road, Shanghai 200438, China

[3]College of Chemistry and Environmental Engineering, Shenzhen University, Shenzhen 518055, China

[4]The Molecular Foundry, Lawrence Berkeley National Laboratory, Berkeley, California 94720, USA

*Corresponding authors: E-mails: yushbo@sioc.ac.cn; zhouw@fudan.edu.cn; ztli@fudan.edu.cn

One Sentence Summary: Porous polymers work as promising protamine surrogates to reverse the anticoagulation of unfractionated and low-molecular weight heparins.

Abstract: Unfractionated heparin (UFH) and low-molecular weight heparins (LMWHs) are widely used anticoagulants for surgical procedures and extracorporeal therapies. However, all of them have bleeding risks. Protamine sulfate, the only clinically approved antidote for UFH, not only has adverse effects, but also only partially neutralizes LMWHs. Here, we report an inclusion-based strategy for efficient neutralization of both UFH and LMWHs by cationic porous supramolecular organic frameworks (SOFs) and porous organic polymers (POPs), which are driven by multivalent electrostatic interactions. Isothermal titration calorimetric and fluorescence experiments revealed that these porous polymers displayed strong binding affinities for both UFH and LMWHs, whereas dynamic light scattering and zeta potential tests supported that the binding took place with the heparins being adsorbed into the interior of the porous hosts. Activated partial thromboplastin time, anti-FXa and thromboelastography assays showed that their efficacy of neutralization was higher than or as high as that of protamine for UFH and generally superior to protamine for LMWHs. Mice tail transection assay and rat *in vivo* neutralization efficacy by aPTT and anti-FXa assays further confirmed the superior ability of **SOF1** and **POP1** as antidote in the treatment of anticoagulant-caused bleeding than protamine. Acute toxicity evaluations with mice revealed that the **SOF1** had a therapeutic index of 28 and displayed outstanding biocompatibility and safety profiles. The results support that porous polymers could supply safe and rapid reversal of UFH and LMWHs and, as protamine surrogates, provide an improved approach for their neutralization.

INTRODUCTION

Heparin is a linear sulfated polysaccharide that consists of repeating disaccharide subunits of α-1,4 linked uronic acid and D-glucosamine. As a family of linear biomolecules with the highest density of negative charges, heparin is widely used as an intravenous anticoagulant which

accelerates the inhibition of antithrombin for serine proteases within the blood coagulation cascade (*1*). Currently, unfractionated heparin (UFH, M_w = ~15 kDa), low-molecular-weight heparins (LMWHs, M_w = 3.6-6.5 kDa), and the synthetic pentasaccharide fondaparinux (M_w = 1.7 kDa) are routinely used to patients clinically. UFH is delivered during acute thrombotic events or procedures that requires extracorporeal circulation (i.e., hemodialysis or cardio-pulmonary bypass) and thus blood fluidity (*2, 3*), while LMWHs and fondaparinux are used to treat and/or prevent deep vein thrombosis and pulmonary embolism (*4, 5*). Despite its widespread application in clinics, UFH-based anticoagulant has a major limitation of the side effect of bleeding, which necessitates an antidote which can neutralize its anticoagulant activity (*6-8*). To date, protamine, a small arginine-rich protein (Mw: ~5 kDa), is the only antidote that is approved to neutralize UFH (*9-11*). This neutralization is fully realized through multivalent electrostatic attraction between its positively charged guanidinium groups and the negatively charged sulfate and carboxylate groups of heparin (*11*). However, protamine only partially neutralizes LMWHs (*12, 13*), with a maximal efficiency of ca. 60%, in case of accidental overdose or serious bleeding caused by LMWHs. Although LMWHs have a more predictable dose response (*1, 14, 15*), the ineffectiveness of protamine and lack of efficient alternate antidotes limit their use for the treatment of thrombotic events (*16*). Apart from its limited efficacy towards LMWHs, the therapeutic use of protamine for the reversal of UFH also has other concerns, which includes toxicities and life-threatening complications (*15, 17-20*), unpredictable dose response and narrow therapeutic window (*12, 13, 21*), as well as the reliability of the supply chain as animal-sourced product for regulatory agencies(*11*). Therefore, the development of efficient, nontoxic, universal antidotes with excellent reversal activity towards heparin-based anticoagulants would be of significantly clinical value.

The past decade has witnessed the test of a number of heparin antidotes(*11, 22-24*), which include small molecules (*25-29*), polymers (*30-33*) as well as proteins (*34, 35*). However, all of these approaches have experienced no clinical success. Given that UFH and LMWHs are all linear anionic polymer or oligomers, the development of their antidotes has largely focused on the utilization of multivalent binding between the cationic groups of antidotes and the anionic groups of the anticoagulants (*36-38*). We envisaged that three-dimensional (3D) polycationic polymers with intrinsic, nano-scaled porosity might provide ideal, conformationally adaptable "pockets" to adsorb and consequently inhibit the anticoagulation of this family of agents. Apart from the endowment of synergetic electrostatic attraction in a 3D space for the achievement of high binding stability, porous polymers can also allow for the scattered distribution of their positive charges and thus avoid their high density on the surface of the structures, which has been a major biocompatibility concern of the polycationic antagonists (*39, 40*).

Here we report the development of a new adsorption-sequestration strategy for the design of universal heparin reversal agents using two families of 3D cationic porous polymers, i.e., supramolecular organic frameworks (SOFs) and porous organic polymers (POPs). We show that both SOFs and POPs were capable of rapidly reversing UFH and three clinically used LMWHs. The efficacy and safety studies using blood coagulation assays and animal models demonstrated that, for all the heparin-based anticoagulants, one SOF agent, with excellent biocompatibility, exhibit higher anticoagulant activity and wider therapeutic window than the clinically used protamine.

RESULTS

Design and synthesis

We previously constructed water-soluble, cationic 3D SOFs through hydrophobically driven co-assembly of tetrahedral molecular blocks and cucurbit[8]uril (CB[8]) (*41, 42*). Such diamondoid SOFs have been revealed to efficiently include short DNA for intracellular delivery (*43*), which is driven by cooperative ion-pairing electrostatic interaction between the pyridinium cations of the frameworks and the phosphate anions of DNA. Since UFH and LMWHs are all linear oligomers that have a density of negative charges (two per monosaccharide unit) two times that of DNA (one per nucleotide unit), we conjectured that these porous polymers would exhibit high ability to include UFH and LMWHs and thus reverse their anticoagulation activity. We thus prepared two SOFs (**SOF1** and **SOF2**) and four POPs (**POP1~POP4**) to explore this potential (Fig. 1).

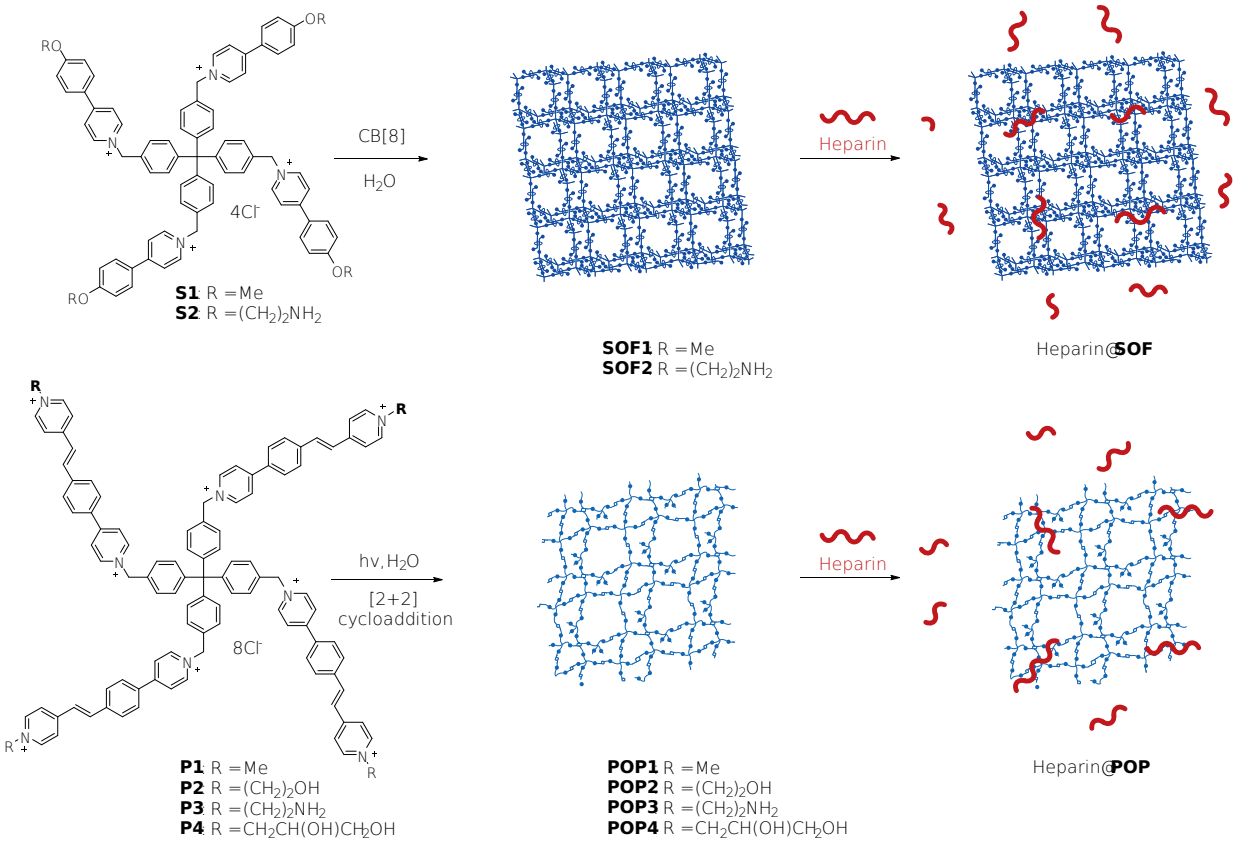

Fig. 1. Construction of **SOF1**, **SOF2** and **POP1~4** and the proposed mechanism for their inclusion and neutralization of UFH and LMWHs.

The preparation of **SOF2**, with a 2.2 nm aperture, from the co-assembly of compounds **S2** and CB[8] (1:2) was performed using the reported method (*41*). For the present study, compound **S1** was further prepared to construct **SOF1** by binding with CB[8] under the identical conditions (Fig. 1). The four hydrophilic aminoethyl groups of **S1** provided it with increased water-solubility, ≥10 mM relative to 2.0 mM of **S2**. The two tetrahedral monomers possess the same rigid backbone. Thus, **SOF1** was expected to possess a regular framework similar to that of **SOF2**. Both ^{1}H NMR and UV-vis titration experiments confirmed the 1:2 binding stoichiometry of **S1** and CB[8] (fig. S1 and S2), while synchrotron small angle X-ray scattering (SAXS) and

diffraction (XRD) experiments supported its framework regularity in both solution and solid state. The SAXS profile obtained for the solution- and solid-phase samples both exhibited a peak centered at 1.61 (fig. S3), which corresponded to the {220} spacing of the modelled diamondoid framework, while the XRD profile recorded for the solution and solid samples displayed peak at d = 1.81 and 1.37 nm, respectively, which matched the {211} and {131} facings calculated for the modelled structure (fig. S4). Dynamic light scattering (DLS) experiments revealed that, at [**S1**] or [**S2**] = 20 μM, the solutions of **SOF1** and **SOF2** gave rise to a hydrodynamic diameter (D_H) of 78.8 and 58.5 nm, respectively (fig. S5), which showed the formation of nano-scaled supramolecular entities in water. At this concentration, the two samples exhibited a zeta potential of 32.7 and 32.0 mV, respectively (fig. S6a and S6b), which supported that both frameworks possessed a positively charged surface. Within the concentration range of 10-70 μM studied, the value was relatively unchanged, which supported that their frameworks at different concentrations maintained a fixed aperture and thus charge density.

POP1 was prepared from visible light-induced intermolecular [2+2] cycloaddition of the 4-styrylpyridinium unit of **P1** according to the reported method (*44*). Three new compounds **P2~P4**, which are all highly soluble in water (≥10 mM), were prepared for investigating the effect of the introduction of hydrophilic side chains on the neutralization capacity of the resulting porous polymers **POP2~4**. Under visible light irradiation, all the three compounds underwent intermolecular [2+2] cycloaddition for the ethene units of the appended aromatic segments. The reactions were tracked using UV-vis spectroscopy, which showed the continual weakening of the diagnostic absorption, which centered at 362 nm, of the 4-styrylpyridinium unit and the appearing of the featured absorption of the resulting cyclobutene derivatives centered at 307 nm (fig. S7). After about seven hours, quantitative conversion could be realized to afford the corresponding soluble porous polymers **POP2~4**. DLS experiments showed that, at [tetrahedral monomers] = 20 μM, the solution of **POP1~4** gave rise to a D_H value of 37.8, 37.8, 32.7, and 37.8 nm (fig. S8). In contrast, the monomers of the identical concentration afforded a D_H of 4.19-5.61 nm, which may be caused by their aggregation driven possibly by hydrophobicity. Within the concentration of 10 μM to 1.0 mM, the D_H of **POP1~4** did not change considerably, reflecting their good stability (fig. S8). The zeta potential of **POP1~4** at the concentration of 20 μM of the monomer were determined to be 28.3, 26.5, 23.2, and 26.0 mV, respectively (fig. S6, c-f). Reducing the concentration to 10 μM or increasing it to 50 μM did not cause important change of the values, which again supported that all the polymers were stable and possessed close charge density on their surfaces. Molecular modelling showed that, when the polymers formed an ideal diamondoid-styled framework, they afforded an aperture of 3.1 nm (fig. S9).

Binding affinity of porous polymers with heparin

Isothermal titration calorimetric (ITC) experiments were first carried out to study the binding affinity of the above porous polymers for UFH and LMWHs, including dalteparin sodium (Dalte), enoxaparin sodium (Enoxa), and nadroparin calcium (Nadro)) in saline or phosphate buffered solution (PBS buffer, pH = 7.4). As a simplified treatment of the complicated binding event, the ITC results were used to derive the apparent binding constants K_a between the tetrahedral building blocks of the polymers and disaccharide repeat units of the heparins by assuming a 1:1 stoichiometry (Table 1, Fig. 2, A-C and fig. S10-S17), as reported for the binding between SOFs and short DNA (*43*). The apparent binding constants were generally high, with the lowest value being 4.99×10^5 M^{-1} for the binding between **SOF1** and Dalte. The results also

showed that, for all the cases studied, the binding was driven both enthalpically and entropically. The enthalpy contribution should come from the multivalent intermolecular ion-pair interactions, while the entropy contribution may be rationalized by considering that the binding led to the inclusion of the linear heparins to the interior of the porous polymers to cover the hydrophobic surfaces of their frameworks, which would cause the release of the high-energy water molecules of low freedom from the hydrophobic surfaces (*43, 45*).

The fluorescence titration experiments in saline were further carried out for **SOF1** and **POP1** with all the four heparins. For **SOF1**, its fluorescence was quenched continuously with the addition of the solution of the heparins and the quenching displayed an inflection at a ratio of 1.8 to 2.2 between the total anionic concentration of the heparins and the total cation concentration of the framework (Fig. 2, D-F and fig. S18). For **POP1**, the fluorescence was strengthened with the addition of the heparins and this strengthening also reached maximum which occurred at a ratio of 1.8 to 2.0 between the total anionic concentration of the heparins and the total cation concentration of the polymer (fig. S19). Given the low concentrations of both samples, these results supported strong binding between them.

Table 1. Thermodynamic parameters for the binding between porous polymers with UFH and LMWHs at 25 °C measured by ITC.

Antidote	Heparin	N [a]	K_a [b] (M^{-1})	ΔG [c] (kcal/mol)	ΔH [c] (kcal/mol)	$-T\Delta S$ [c] (kcal/mol)
SOF1 [d]	UFH	1.86 ± 0.002	1.19 (± 0.22) × 10^6	-8.29 ± 0.058	-3.96 ± 0.058	-4.32
	Dalte	1.51 ± 0.016	4.99 (± 0.60) × 10^5	-5.48 ± 0.039	-3.20 ± 0.039	-2.29
	Enoxa	1.62 ± 0.011	3.91 (± 0.88) × 10^6	-9.00 ± 0.006	-4.47 ± 0.006	-4.53
	Nadro	1.90 ± 0.034	6.55 (± 1.69) × 10^5	-7.93 ± 0.100	-4.03 ± 0.100	-3.90
SOF2 [e]	UFH	0.73 ± 0.009	3.22 (± 0.81) × 10^6	-8.89 ± 0.062	-3.20 ± 0.062	-5.69
	Dalte	0.77 ± 0.009	5.03 (± 1.37) × 10^6	-9.13 ± 0.066	-3.68 ± 0.066	-5.45
	Enoxa	0.73 ± 0.004	3.11 (± 1.15) × 10^7	-8.74 ± 0.052	-3.11 ± 0.052	-5.63
	Nadro	1.09 ± 0.190	5.44 (± 0.11) × 10^5	-7.82 ± 0.150	-6.01 ± 0.150	-1.81
POP1 [d]	UFH	1.20 ± 0.019	1.81 (± 0.32) × 10^6	-8.53 ± 0.120	-5.31 ± 0.120	-3.22
	Dalte	1.15 ± 0.007	2.61 (± 0.26) × 10^6	-8.76 ± 0.052	-5.72 ± 0.052	-3.04
	Enoxa	1.22 ± 0.011	1.80 (± 0.21) × 10^6	-8.53 ± 0.086	-6.94 ± 0.086	-1.59
	Nadro	1.75 ± 0.019	1.11 (± 0.15) × 10^6	-8.24 ± 0.075	-5.42 ± 0.075	-2.82
POP2[d]	UFH	0.81 ± 0.004	2.11 (± 0.24) × 10^6	-8.60 ± 0.037	-4.56 ± 0.037	-4.04
	Dalte	1.14 ± 0.003	6.40 (± 0.27) × 10^5	-7.95 ± 0.015	-4.53 ± 0.015	-3.39
	Enoxa	0.94 ± 0.005	6.19 (± 0.48) × 10^5	-6.74 ± 0.044	-5.71 ± 0.044	-2.18
	Nadro	1.08 ± 0.004	3.85 (± 0.19) × 10^5	-7.16 ± 0.025	-5.01 ± 0.025	-2.60
POP3 [d]	UFH	0.70 ± 0.004	4.34 (± 0.90) × 10^6	-10.23 ± 0.042	-3.37 ± 0.042	-5.67
	Dalte	0.69 ± 0.004	3.32 (± 0.51) × 10^6	-9.79 ± 0.037	-3.65 ± 0.037	-5.23
	Enoxa	0.74 ± 0.006	3.08 (± 0.58) × 10^6	-9.07 ± 0.054	-4.33 ± 0.054	-4.51
	Nadro	0.99 ± 0.011	1.68 (± 0.39) × 10^6	-8.99 ± 0.067	-4.05 ± 0.067	-4.43
POP4 [d]	UFH	0.36 ± 0.003	2.26 (± 0.32) × 10^6	-8.78 ± 0.060	-4.42 ± 0.060	-4.22
	Dalte	0.93 ± 0.005	1.94 (± 0.22) × 10^6	-8.63 ± 0.036	-4.50 ± 0.036	-4.07
	Enoxa	0.93 ± 0.007	8.15 (± 0.87) × 10^5	-7.34 ± 0.053	-5.27 ± 0.053	-2.78
	Nadro	1.17 ± 0.014	1.10 (± 0.27) × 10^6	-8.33 ± 0.076	-4.45 ± 0.076	-3.77

[a] N is the number of the ligand-binding sites per macromolecule. [b] K_a is the binding constant for the interaction between antidote and heparin. [c] ΔG, ΔH and $-T\Delta S$ were calculated per mole of the tetrahedral units of the polymers for one disaccharide unit of the heparins. [d] Heparins were titrated into antidotes at 25 °C in saline. [e] Heparins were titrated into the antidotes at 25 °C in water.

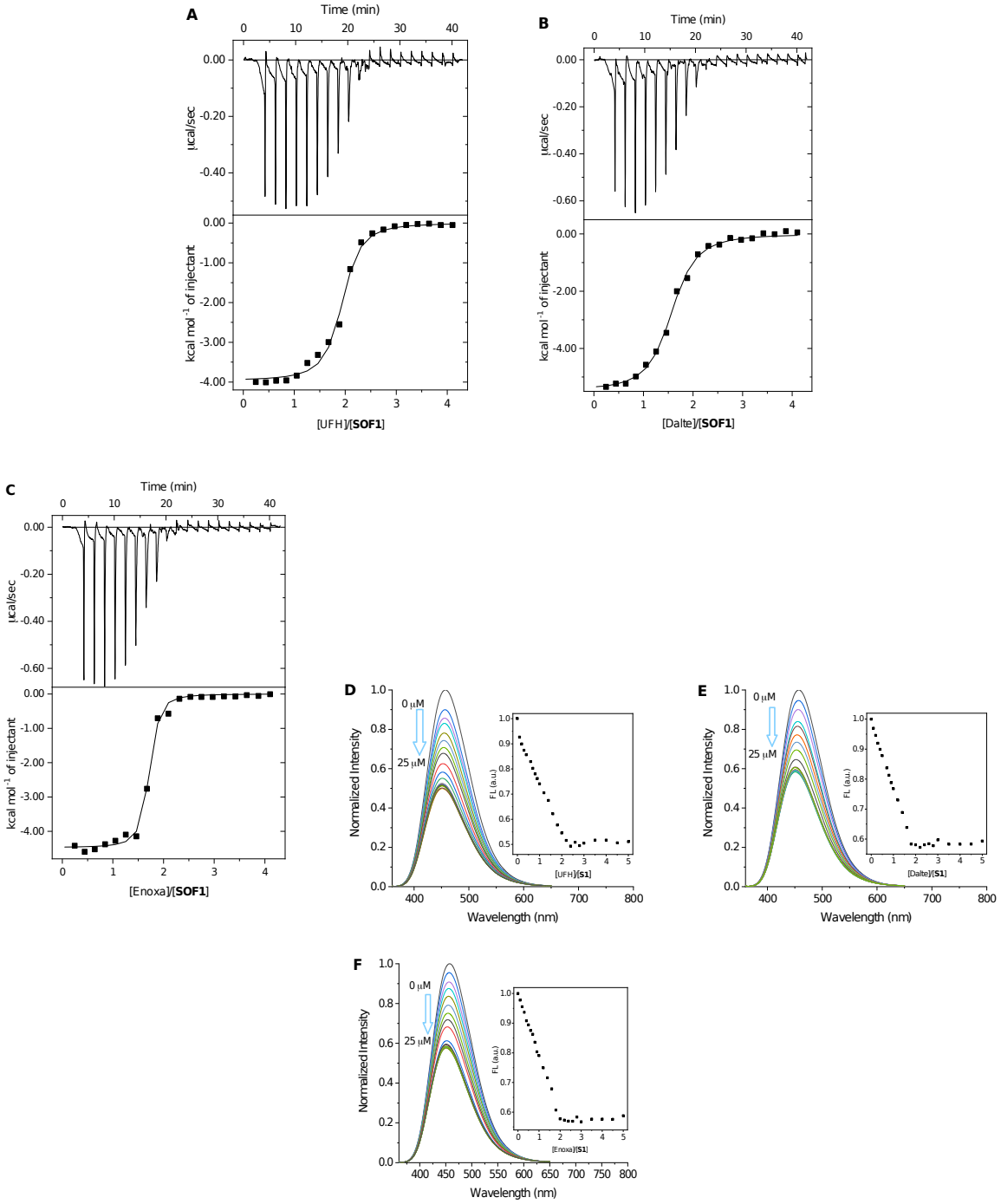

175 **Fig. 2.** Isothermal titration thermograms recorded by adding the solution of (**A**) UFH, (**B**) Dalte and (**C**) Enoxa ([disaccharide unit] = 0.4 mM) into the solution of **SOF1** ([**S1**] = 50 μM) at 25°C in saline. The solid lines represent the best non-linear fit of the data to a 1:1 binding model. Fluorescence spectra of the solution of **SOF1** ([**S1**] = 5 μM) in saline with the addition of (**D**) UFH, (**E**) Dalte and (**F**) Enoxa in saline ([disaccharide unit] = 0-25 μM). The excitation and emission wavelength were 340 nm and 457 nm, respectively. Inset: plot of [heparin]/[**S1**] versus
180 changes of normalized intensity.

Binding mechanism of porous polymers with heparin

To get insight into the mechanism of binding between the porous polymers and heparins, DLS experiments were further conducted for the solutions of the polymers with the addition of the heparins. At the concentration of 60 μM disaccharide unit, all the four heparins gave a very small D_H of ≤ 3 nm (fig. S20a), which showed that these highly soluble polysaccharides did not aggregate in water. When the heparins of the same concentration were added to the solution of **SOF1** ([**S1**] = 20 μM), the DLS profile of the resulting mixture solutions did not display this small peak of the heparins. In contrast, the mixture still gave the peak of the polymers with the D_H value being determined to be 78.8, 85.2, 82.3, and 70.6 nm, respectively, for UFH, which matched that (78.8 nm) of the solution of **SOF1** of the same concentration, well supporting that the heparins were included into the interior of the framework. The increase, with Dalte and Enoxa, or decrease, with Nadro, of the value might reflect the expanding or shrinking of the polymer frameworks after including the heparins. Similar results were also observed for the mixtures of **SOF2** and **POP1~4** and the four heparins (fig. S20).

At the concentration of 20 μM, the aqueous solution of UFH, Dalte, Enoxa, and Nadro gave rise to a negative zeta potential of -22.0, -27.9, -30.0 and -19.5 mV, respectively (fig. S6). Adding the aqueous solution of the six polymers to the solution of the heparins caused the zeta potential to increase continuously. At the concentration of 15 μM for **SOF1**, 30 μM for **SOF2** and 20 μM for the four POPs, the zeta potential reached that of the solution of the respective polymer, and kept unchanged with further increase of the concentration. This result provided solid evidence to support that the linear heparins were completely included into the interior of the polymers, rather than adhered to their surfaces, at a high enough concentration. Moreover, after including the heparins, the surfaces of the polymers were unchanged and thus maintained their charge density as that of the polymers themselves.

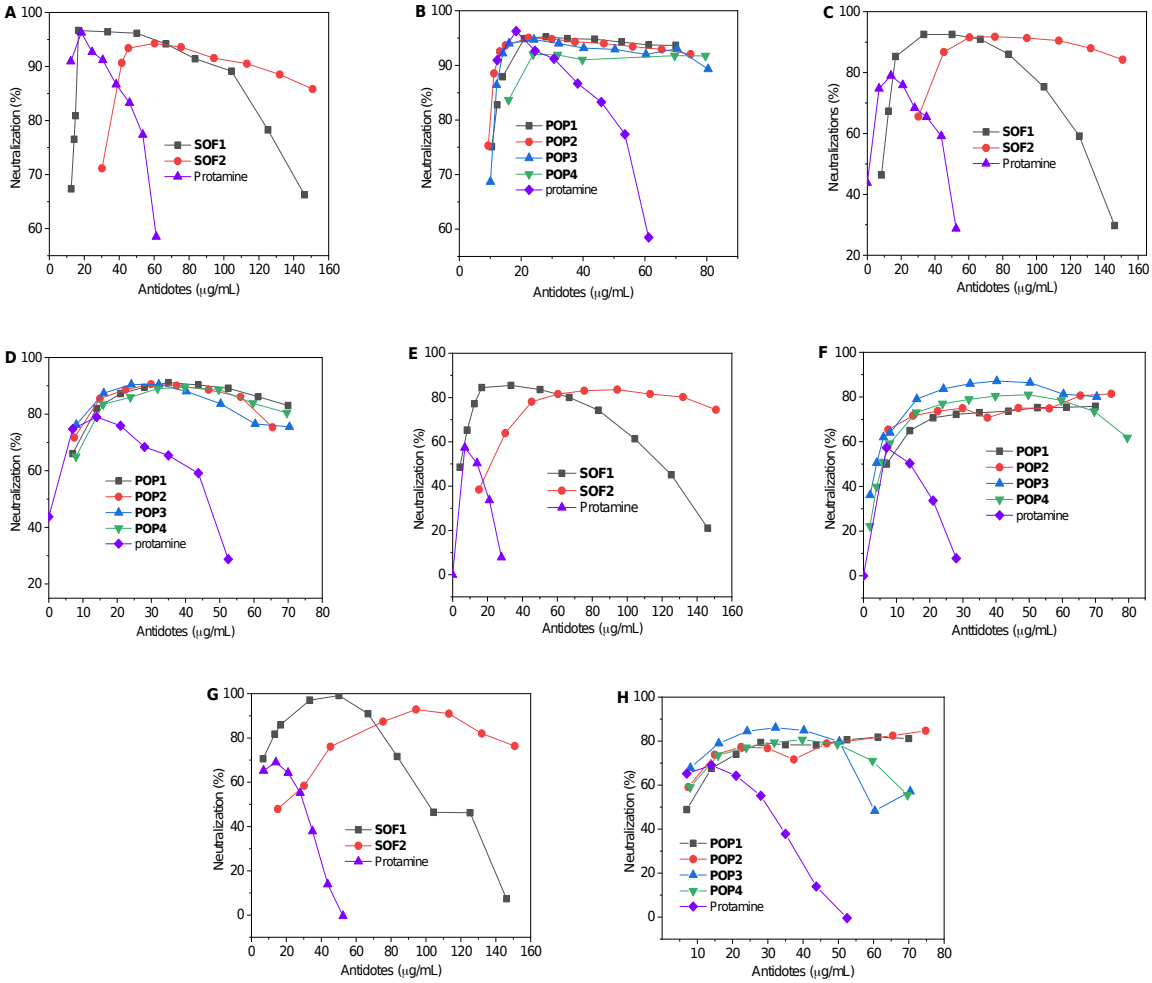

Fig. 3. APTT assays in human plasma for the neutralization of (**A** and **B**) UFH (2.48 IU/mL), (**C** and **D**) Dalte (2.52 IU/mL), (**E** and **F**) Enoxa (2.56 IU/mL), and (**G** and **H**) Nadro (1.76 IU/mL) by SOFs and POPs. The aPTT values were measured by full-automatic blood coagulation analyzer. The heparin neutralization efficacy was calculated from the standard curves which were plotted with the aPTT value obtained from a series of heparinized-PPP that prepared by incubating different concentration of heparins into PPP (1/99, v/v), resulting the final concentration of heparinized-PPP to be in the range of 0.078-4.0 IU/mL.

In vitro efficacy assessments by activated partial thromboplastin time assay

The above ITC, fluorescence and DLS experiments confirmed the high binding affinity of the SOFs and POPs towards both UFH and LMWHs. We thus systematically assessed the *in vitro* ability of these porous polymers to neutralize the four heparins by testing the activated partial thromboplastin time (aPTT) in both human and bovine plasma. High doses of UFH (2.48 IU/mL), Dalte (2.52 IU/mL), Enoxa (2.56 IU/mL) and Nadro (1.76 IU/mL) were used to mimic the anticoagulant overdose situation (*30*). Heparinized human plasmas were treated with increasing doses of the SOFs and POPs to evaluate their neutralization activity (Fig. 3, and table S1). For comparison, the activity of protamine was also determined for all the four heparins under the identical experimental conditions. The aPTT assays in human platelet poor plasma (PPP) showed that all the six porous polymers could efficiently neutralize UFH in a dose-dependent manner (Fig. 3). **SOF1** and **SOF2** reached the top activity at the concentration of 17

and 60 μg/mL, respectively, and could retain over 90% neutralization activity from 17 to 85 μg/mL and from 42 to 94 μg/mL, respectively (Fig. 3A). Within the dose range of 20 to 70 μg/mL, **POP1~4** also displayed over 90% neutralization activity (Fig. 3B). Although the neutralization slightly lowered after reaching the top activity, the therapeutic concentration window of all the six agents was quite broad. In contrast, whereas protamine fully neutralized UFH at the dose of 18 μg/mL, the neutralization activity rapidly decreased at concentrations greater than it (Fig. 3A), which was consistent with the fact that protamine has the drawback of narrow therapeutic window (*9-11*). The top neutralization activity of protamine for Dalte, Enoxa and Nadro, the three most widely used LMWHs in the clinic, was determined to be 78%, 57% and 69%, respectively (Fig. 3, B-D), well reflecting the fact that protamine only partially reverse the effect of LMWHs (*7*). As expected, greater concentrations of protamine continuously caused quick decrease of its neutralization activity (Fig. 3, B-D), which is again consistent with its unpredictable dose response and narrow therapeutic window. However, all the six porous antidotes could realize a top neutralization activity of 84%-99% (table S1), which was considerably higher than that of protamine related to the respective heparin. Moreover, all the agents retained the high neutralization activity within a relatively wide concentration window. Compared with **SOF2**, for all the four heparins, **SOF1** exhibited a superior or comparable neutralization activity even at a substantially lowered dose (Fig. 3, A, C, E and G). This difference might be rationalized by considering that the appended amino group of **S1** formed additional hydrogen bonding with the anion or hydroxyl groups of the heparins and thus increased the binding affinity of **SOF1** toward heparins through enhanced multivalent inclusion.

The neutralization activity of the porous antidotes for both UFH and LMWHs was also assessed in bovine PPP using aPTT assays (fig. S21 and table S2). The results showed that, for both UFH and LMWHs, the top neutralization activity of the porous antidotes was also generally superior over that of protamine. Moreover, in all the cases studied, the two kinds of antidotes all displayed a wider concentration window while reaching a neutralization activity higher than that of protamine.

In vitro efficacy assessments by chromogenic anti-FXa assays

The potentiation of thrombin inhibition (anti-IIa activity, also prolongation of activated partial thromboplastin time) requires at least 18 saccharide units in the chain (MW: ca. 5400 Da), whereas the acceleration of the inhibition of factor Xa (anti-FXa activity) requires only a pentasaccharide sequence (MW: ca. 1700 Da). Accordingly, LMWHs preferentially inhibit factor Xa and only to a low extent thrombin and aPTT (*46, 47*). We thus further conducted the chromogenic anti-FXa assay to investigate the neutralization activity of the new porous antidotes. As the above aPTT experiments revealed that the neutralization activity of **SOF1** was generally higher than **SOF2**, and four POPs were very comparable, we therefore chose **SOF1** and **POP1** to conduct the chromogenic anti-FXa assay. Firstly, blood compatibility of antidotes was tested by anti-FXa assay in human PPP, which showed that **SOF1** and **POP1** did not cause any observable effect on the anti-FXa activity (fig. S22). The ability of the two antidotes, as well as protamine, for the neutralization of UFH and Dalte was then measured and the results are summarized in Fig. 4A and 4B. Under the identical experimental conditions, protamine showed the top anti-FXa activity of 92% toward UFH and 60% toward Dalte, at the dose of 21 or 60 μg/mL, respectively. Both **SOF1** and **POP1** surpassed protamine within a large concentration window. For UFH (Fig. 4A), at concentrations from 16 μg/mL to 160 μg/mL or from 21 μg/mL

to 70 μg/mL, **SOF1** and **POP1** could achieve ≥96% and ≥95% of neutralization, respectively. For Dalte (Fig. 4B), at concentrations from 94 μg/mL to 170 μg/mL or from 35 μg/mL to 70 μg/mL, both agents could achieve ≥80% of neutralization and the top neutralization of 91% or 94% at the large dose of 150 μg/mL or 70 μg/mL.

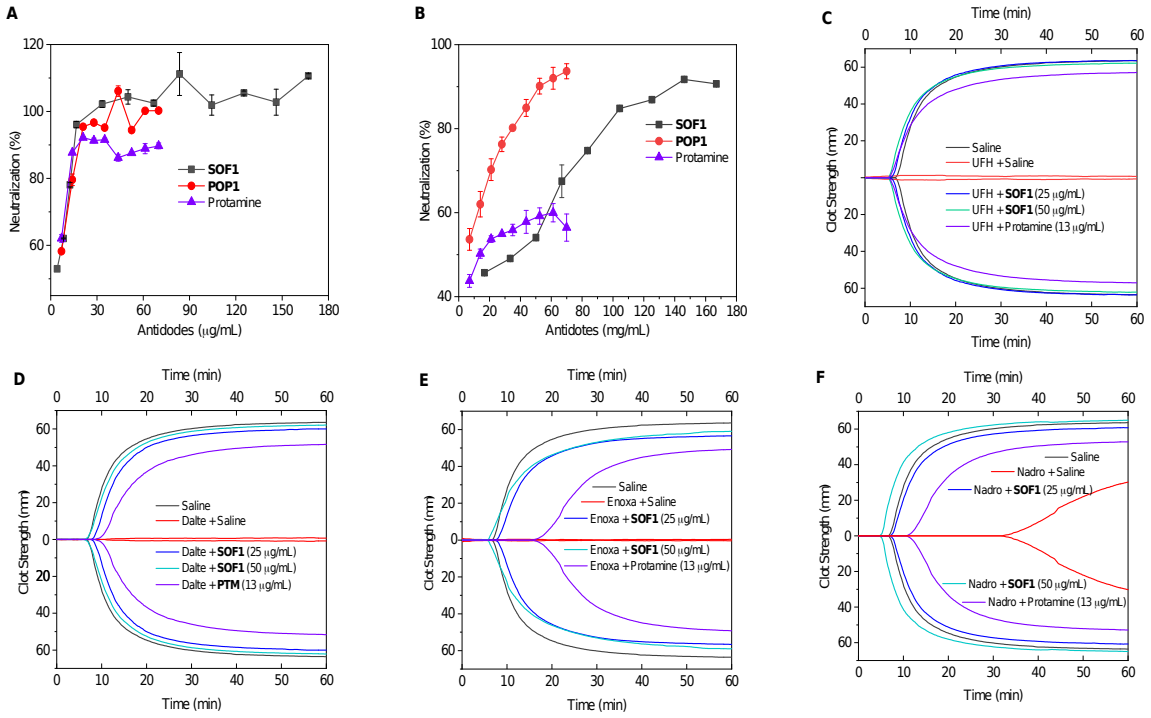

Fig. 4. Neutralization of (**A**) UFH (2.48 IU/ml), and (**B**) Dalte (2.52 IU/ml) in saline by anti-FXa assay in human plasma, with the gradually adding of **SOF1**, **POP1** and protamine, respectively; data are presented as means ± SD. Neutralization of (**C**) UFH (2.48 IU/mL), (**D**) Dalte (2.52 IU/mL), (**E**) Enoxa (2.56 IU/mL), and (**F**) Nadro (1.76 IU/mL) by **SOF1** in human whole blood measured by TEG assays.

In vitro efficacy assessments thromboelastographic assays

The validation of **SOF1** and **POP1** for the neutralization of UFH and LMWHs under an approximately physiological condition was also investigated using thromboelastographic (TEG) assays in human whole blood (HWB) (*48*). The clot characteristics of the heparinized HWBs were assessed with the addition of the porous antidotes of varying concentrations. Guided by the top neutralization dose in aPTT assays, the concentration of the antidotes used for these TEG assays were set as 25 and 50 μg/mL for **SOF1**, 13 and 26 μg/mL for **POP1**, and 13 μg/mL for protamine. Salinized HWB from five donors was used as the normal control (Fig. 4, C-F, fig. S23, and table S3). The addition of the heparin all significantly changed the clotting characteristics of the blood samples. Coagulating time was as long as more than 118 min, whereas clotting strength (maximum amplitude) lowered to 0 mm, with Nadro as exception which was not able to fully anticoagulate the blood (Fig. 4F). The TEG assays showed that, at the dose of 25 or 50 μg/mL, **SOF1** could completely reverse the anticoagulant effect of both UFH and all three LMWHs and restore blood clot properties to normal (Fig. 4, C-F and table S4). At the dose of 13 μg/mL which achieved the top neutralization activity for the heparins as revealed by the above aPTT assay, protamine could also fully reverse the anticoagulant effect of

UFH (Fig. 4C and table S5). However, for the anticoagulation activity of the three LMWHs, only partial reversal was observed (Fig. 4, D-F and table S5). These observations were consistent with the above results obtained with the aPTT and chromogenic anti-FXa studies. At the dose 26 μg/mL, **POP1** could also completely reverse UFH, but for LMWHs, it did not (fig. S24 and table S6).

***In vivo* efficacy assessments by tail transection assay in mice**

The *in vitro* activities established by the above aPTT, anti-FXa and TEG assays revealed that **SOF1** and **POP1** were efficient antidotes for both UFH and LMWHs. Their efficacy was further assessed using mouse tail transection assay (bleeding model). In the tail transections assay, ICR mice were used to study the heparin neutralization activity and possible bleeding side effect (Fig. 5a). ICR mice were randomly distributed to nine groups (n = 10 per group, five male and five female): i) saline alone (normal group); ii) heparin (UFH (248 IU/kg) or Dalte (252 IU/kg)) + saline; iii) heparin (UFH (248 IU/kg) or Dalte (252 IU/kg)) + **SOF1** (3.34 mg/kg) or **POP1** (2.60 mg/kg); iv) heparin (UFH (248 IU/kg) or Dalte (252 IU/kg)) + protamine (2.60 mg/kg). The normal group was given two intravenous injections of saline, whereas other groups were given an injection of heparin followed by an injection of saline or one of the two antidotes in five minutes. The bleeding behavior versus time was measured according to previously reported method with modifications (*49*). The bleeding time was recorded until there was no blood spot on the filter paper visible to naked eyes and the blood loss was measured by the absorbance (405 nm) of the blood cell lysis in 10 wt% NaOH solution, and calculated by fitting to the standard curve (fig. S25).

As shown in Fig. 5B-5E, and table S7, the average bleeding time and blood loss volume of the control groups treated with UFH or Dalte vigorously increased, with the values to be 60.80 ± 9.56 min and 243.21 ± 58.77 μL for UFH, 64.20 ± 9.46 min and 206.27 ± 48.95 μL for Dalte, respectively, which were much higher than the normal control (21.40 ± 3.02 min and 24.22 ± 7.45 μL, respectively). Moreover, a significant individual difference was observed in both UFH and Dalte groups, which was consistent with the less predictable dose response of heparins in clinic. In UFH neutralization, the mice injected with protamine did not show any significant difference in bleeding time and blood loss compared to those in the normal group and a major individual deviation was also observed (Fig. 5, B and C, and table S8). In comparison, treating the mice with **SOF1** or **POP1** significantly reduced the bleeding time and blood loss to the normal level, with no significant difference *vs.* the normal group (P = 0.2919 and 0.8066, respectively). Similar results were obtained for Dalte reversal (Fig. 5, D and E, and table S9), the bleeding time and blood loss of **SOF1** and **POP1**-treated groups showed a very significant difference with Dalte control group (P = 0.0017 and 0.0035), with the average bleeding time and blood loss to be 21.30 ± 2.92 min and 18.93 ± 6.75 μL for **SOF1**, and 18.20 ± 2.46 min and 21.07 ± 8.27 μL for **POP1**, respectively. In contrast, protamine could only partially neutralize Dalte *in vivo*, with the bleeding time of protamine-treated group exhibited weak "no significant difference" with the negative control group (P = 0.2540) and very significant difference with the normal saline group (P = 0.0035). The blood loss also exhibited both very weak "no significant difference" with the Dalte control group (P = 0.1052) and with the normal saline group (P = 0.0850), indicating relatively moderate neutralizing activity of protamine *in vivo* toward Dalte. More importantly, **SOF1** and **POP1-**treated groups had fewer individual deviations when compared with those treated with protamine. These results obtained with mice tail transection

assay strongly supported that both **SOF1** and **POP1** could effectively reverse UFH and Dalte *in vivo*, with more predictable dose responses than protamine.

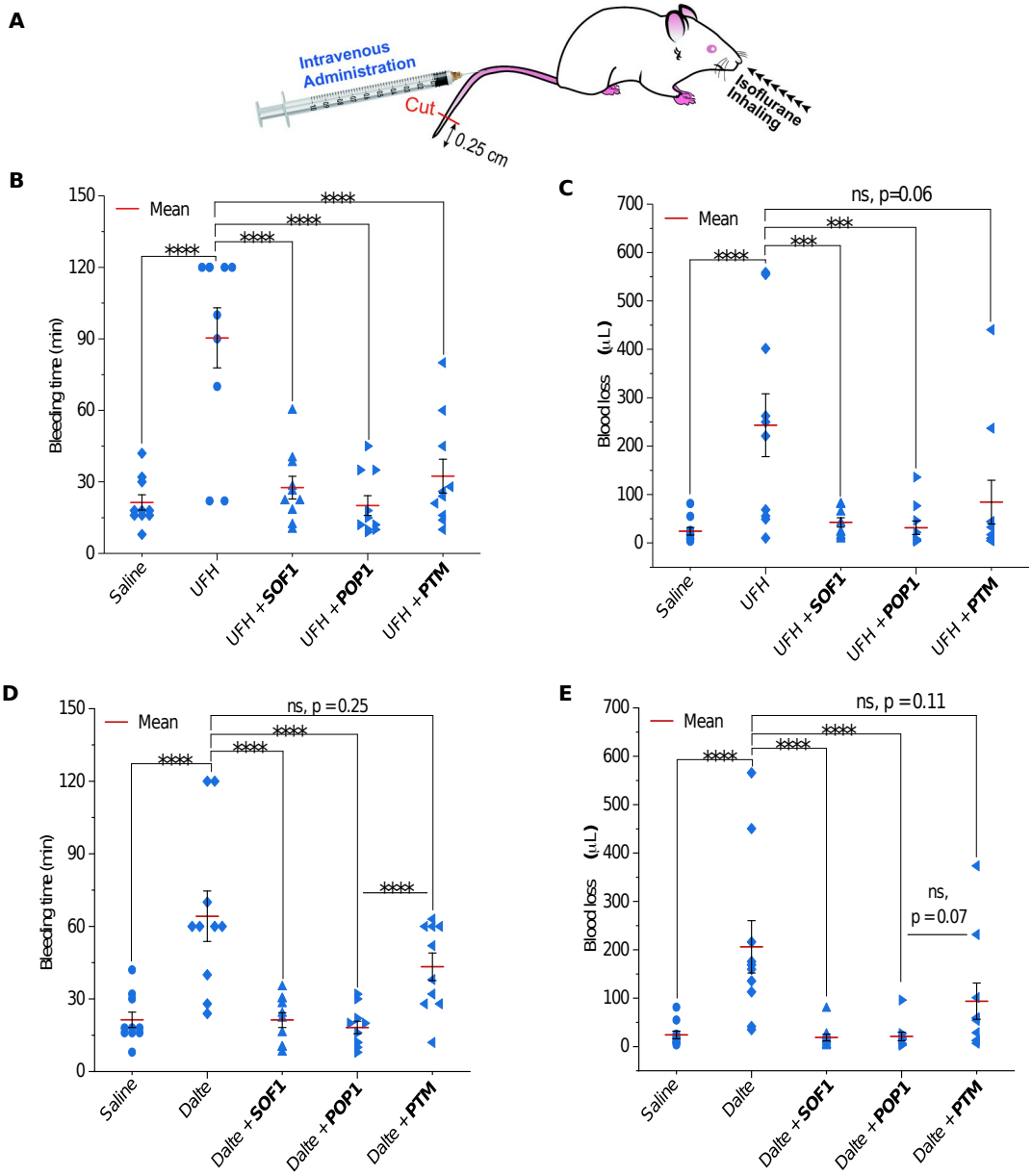

Fig. 5. ***In vivo*** **heparin neutralization via tail bleeding model in ICR mice.** (**A**) A schematic illustration of the mice tail transection model. (**B** and **D**) Total time of bleeding and (**C** and **E**) blood loss volume. All of those models were two-time intravenous (i.v.) administration successively via tail intravenous vein, with the first injection of saline (normal control), or UFH (248 IU/kg) or Dalte (254 IU/kg) at t = 0 min, and followed by saline, or **SOF1** (3.34 mg/kg) or **POP1** (2.6 mg/kg), or protamine (**PTM**, 2.6 mg/kg) at t = 5 min. The distal 2.5 mm of the mouse tail was transected at t = 10 min, blood bleeding time and blood loss were then recorded. Data presented are the means ± S.E.M. (n = 10). *p < 0.05, ***p < 0.01 ****p < 0.005, and ns represents "no significant difference" between the experimental group and the control group. S.E.M.: standard error of mean.

In vivo efficacy assessments by aPTT and anti-FXa assay in Sprague-Dawley rats

Further *in vivo* neutralization efficacy was conducted by aPTT assay and anti-FXa assay in Sprague-Dawley rats by drawing blood from the jugular intravenous vein (Fig. 6A). For this experiment, rats were randomly distributed to five groups for *in vivo* aPTT assay (n = 6 per group, half male and female): i) saline alone (normal group), ii) UFH (248 IU/kg) + saline, iii-v) UFH + **SOF1** (3.34 mg/kg), **POP1** (2.60 mg/kg), or protamine (2.6 mg/kg). For *in vivo* anti-FXa assay (n = 4, half male and female), randomly distributed four groups included: i) Enoxa (256 IU/kg) + saline, ii-iv) Enoxa + **SOF1** (3.34 mg/kg), **POP1** (2.60 mg/kg), or protamine (2.6 mg/kg).

Blood samples of 0 minute were drawn from the jugular vein prior to the first injection from the tail vein, and the second injection was injected five minutes after the first injection. The internal coagulation process was monitored via blood drawing at various time points from the jugular vein.

All blood samples were anticoagulated using 3.8 wt% sodium citrate and were immediately centrifuged to avoid hemolysis. Fresh plasma for each time point was isolated for aPTT and anti-FXa assays. As shown in Fig. 6B and table S10, UFH showed an immediate response with the aPTT exceeding the maximum detection limit (180 s) of the coagulation analyzer, followed by a slow physiological metabolism *in vivo*. It can be seen that the injection of **SOF1**, **POP1** or protamine could all rapidly and completely neutralize UFH within 5.0 min. However, for Enoxa neutralization, **SOF1** showed an activity generally superior over that of **POP1** or protamine. Notably, **SOF1** could reverse over 85% anti-FXa activity of Enoxa, while **POP1** and protamine reversed about 60% (Fig. 6C, table S11). This *in vivo* neutralization results showed that the superior heparin reversal activity of **SOF1** observed *in vitro* could be effectively translated *in vivo*.

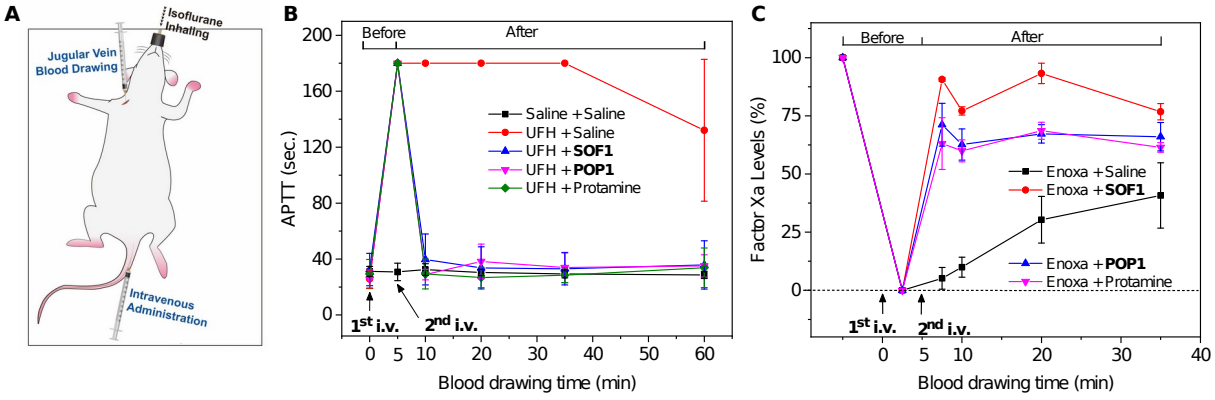

Fig. 6. *In vivo* neutralization toward UFH and Enoxa in Sprague-Dawley rats. (**A**) A schematic description of the rat model for i.v. administration and jugular vein blood drawing. (**B**) Neutralization of UFH by **SOF1**, **POP1** or protamine measured with aPTT assay. Rats (n = 6 per group) were i.v. administrated successively with the first injection of saline, or UFH (248 IU/kg) at t = 0 min (1st i.v.), and followed by saline, **SOF1** (3.34 mg/kg), **POP1** (2.6 mg/kg), or protamine (2.6 mg/kg) at t = 5 min (2nd i.v.). The blood was drawn at t = 0, 5, 10, 20, 35, and 60 min. The neutralization efficacy was monitored by aPTT. (**C**) Neutralization of enoxaparin by **SOF1**, **POP1** or protamine in rats measured with the anti-FXa assay. Rats (n = 4 per group) were i.v. administration successively with Enoxa (252 IU/kg) followed by saline at t = 0 min (1st i.v.), **SOF1** (3.34 mg/kg), **POP1** (2.6 mg/kg), or protamine (2.6 mg/kg) at t = 5 min (2nd i.v.). The blood was drawn at t = 0, 2.5, 7.5, 10, 20, and 35 min. Then the factor Xa levels were monitored by BIOPHEN two stage anti-FXa kits. All data are presented as the means ± SD. SD: standard derivation.

Biocompatibility and *in vivo* safety evaluation

As *in vivo* studies supported that **SOF1** and **POP1** could neutralize heparins effectively, we then conducted the dose tolerance studies to assess their toxicity. ICR mice were administered intravenously through the tail vein with a single-bolus of an escalating dose of **SOF1** or **POP1** saline solution. The mice were observed over seven days for any toxic symptoms, and the lethality was recorded (tables S12 and S13). The maximum tolerated dose (MTD) of **SOF1** and **POP1** was 71.2 and 15.6 mg/kg, respectively. SPSS probit model was then used to calculate the probability of dose-dependent toxicity, and the LD_{50} of **SOF1** and **POP1** was estimated to be 92.5 and 20.3 mg/kg, respectively. LD_{50} and corresponding therapeutic dose (3.3 mg/kg for **SOF1**, 2.6 mg/kg for **POP1**) were used to calculate their therapeutic index (TI), giving the value of 28 and 7.9, respectively. Acute toxicity assays were further performed with seventy ICR mice. Single-injection was administrated through the intravenous tail vein with saline or the escalating dose of antidotes (**SOF1** (3.3, 15.7, 31.3, and 62.6 mg/kg) or **POP1** (2.6 and 5.2 mg/kg)). The mice were fed and monitored over 15 days for their body weight changes, mortality, or any signs of acute toxicity. The mice administrated with a varied dose of **SOF1** or **POP1** were less active in the first two days with the weight slightly descended, but grew normally in the following days and even caught up with the normal saline control group (Fig. 7, A and D, tables S14 and S15). Fifteen days after the administration, the mice were euthanized for blood collecting and representative organs (heart, liver, spleen, lungs, kidneys and thymus) harvesting. The organ indexes for **SOF1** and **POP1**-treated mice were comparable to those of the mice treated with saline (Fig. 7, B and E, tables S16 and S17), except for the slight significant difference of liver indexes (Fig 7E) of the mice treated with **POP1** at the dose of 5.2 mg/kg. In addition, the liver and kidney damage indices, including blood urea nitrogen (BUN) and alanine aminotransferase (ALT) levels in serum, also exhibited no significance difference with the saline control (Fig. 7, C and F, tables S18 and S19). Further histopathological analysis of tissue sections from the above treated mice were also conducted to supplement the acute toxicity data. H&E results also indicated no apparent difference between the tissues treated with saline control and **SOF1** or **POP1**, and no sign of tissue abnormality was detected (Fig. 7G and fig. S27 and S27). The above results all suggested that both **SOF1** and **POP1** were safe under therapeutic doses for heparin neutralization, while **SOF1** exhibited an even higher mice tolerance dose and therapeutic index than **POP1**.

Additional biocompatibility studies, including TEG, hemolysis assays as well as cell viability, were then further conducted. TEG was considered more suitable for the biocompatibility test than other *in vitro* coagulation tests as the whole blood containing all the blood components was close to *in vivo* conditions. The TEG traces for **SOF1** were almost identical with that of the healthy donors and the saline control. Furthermore, coagulation parameters such as clotting time and clot strength did not show important change when incubated with **SOF1** at different concentrations (Fig. 7H). The hemolytic effect of **SOF1** was assessed in human and rat red blood cells (RBC), showing that **SOF1** did not exhibit important hemolytic activity (< 3% lysis) within the concentration range of 0-757.6 μg/mL (Fig. 7I), which was much higher than the therapeutic dose range (16.7-33.4 μg/mL) as indicated by the aPTT assays. In contrast, protamine causes very significant erythrocyte hemolysis, as reported in the literature (*30*). The safety of **SOF1** was also verified by cell cytotoxicity through normal cardiac myoblast of rat heart cells and human breast cancer cells (MCF-7) (fig. S28). **SOF1** showed very low cytotoxicity to H9C2 and MCF-7

cells, and the half-maximal inhibitory concentration (IC_{50}) was estimated to be 386.8 μg/mL by H9C2 and 262.4 μg/mL by MCF-7. These values were also much higher than the therapeutic dose of **SOF1** for neutralizing the heparins.

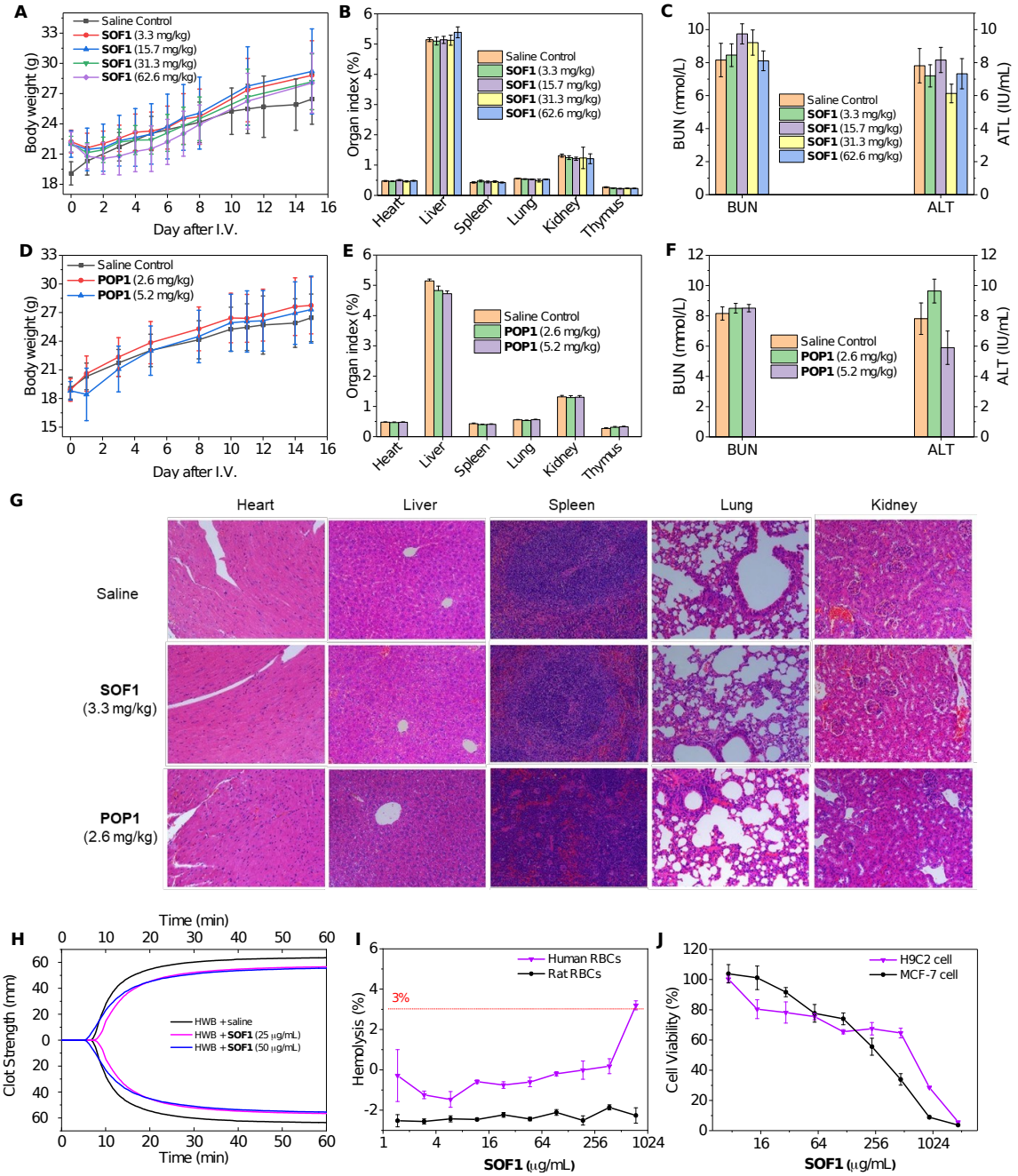

Fig. 7. Preliminary *in vivo* safety and biocompatibility evaluation. (**A-G**) acute toxicity evaluations on different dose of **SOF1** and **POP1**. (**A** and **D**) Weight changes of mice after i.v. administration with a single dose of **SOF1** (**A**) and **POP1** (**D**). (**B** and **E**) Major organ indexes of the mice on day 15 post-administration with **SOF1** (**B**) and **POP1** (**E**). (**C** and **F**) Renal and hepatic functional biomarkers in the blood samples collected from the mice on day 15 after i.v. administration of **SOF1** (**C**) and **POP1** (**F**). Data are presented as mean; S.E.M.; n = 5 for each female or male mice group. (**G**) Representative pathological morphology of main organ after 15 days post administration of saline, **SOF1** (3.3 mg/kg) and **POP1** (2.6 mg/kg). Tissues were stained with hematoxylin and eosin and observed under light microscope (magnification, ×200). (**H**) TEG traces of **SOF1** (25 and 50 μg/mL) in human whole blood. (**I**)

Hemolysis results of **SOF1** was conducted on 5% human and rat red blood cells. (**J**) Cell viability assays of H9C2 cells and MCF-7 cells versus the incubation concentration of **SOF1**. The cells (~1 × 10^4 per well) were incubated with the frameworks at 37 ˚C for 24 h. The viability was evaluated by CCK-8 proliferation tests. Error bars represent the standard deviation for each point.

DISCUSSIONS

We have presented the potential of two kinds of cationic porous organic polymers as new effective antidotes for reversing the anticoagulation of both UFH and three LMWHs. **SOF1** worked as effectively as protamine sulfate in neutralizing UFH and more efficacious towards LMWHs than protamine. For all the four heparins, **SOF1** exhibited an obviously wider concentration window than protamine. Protamine has a very narrow therapeutic window, which makes it less predictable and frequently causes bleeding due to overdose. One important advantage of the new porous antidotes is that their therapeutic windows are generally considerably wider, which should help to reach a high predictability for practical use. **SOF1** has a relatively high TI of 28 and MTD of 71.2 mg/kg. It does not show hemolysis at a dose much higher than that of efficient neutralization of the heparins. These observations indicate that this homogeneous polymer has a good biocompatibility and thus the potential for further evaluation of preclinical studies. Previous study supports that SOFs include DNA through multivalent electrostatic attractions. Since heparins possess an even higher negative charge density, we propose that SOFs and POPs neutralize heparins through including the heparins into the interior of their pores which is also driven by the electrostatic attraction between the positive charges of the porous antidotes and the anionic charges of the heparins. The intrinsic nano-scaled porosity of the antidotes should facilitate this interaction because the inclusion does not require the deformation or transformational change of the polymer backbones. The porosity of the polymeric antidotes also features relatively uniform distribution of their positive charges, which may be an important factor that leads to their relatively low toxicity. As synthetic agents, the porous antidotes are also very stable in water, can be stored at room temperature for months. They can also avoid the potential limitation of livestock, source dependent biological contamination, and probably immunogenic problem. Generally, we provide *in vitro* and *in vivo* evidences to demonstrate that **SOF1** is a very promising candidate as protamine surrogate.

SOFs are self-assembled through the encapsulation of CB[8] for the intermolecular dimers formed by the appended aromatic arms of the tetrahedral building blocks. CB[8] has been evaluated to be of low toxicity (*50*) and its pharmacokinetics with oral administration has been conducted (*51*), which reveals its absorption from gastrointestinal tract into the blood stream is very low. However, the pharmacokinetics with i.v. administration is not available, and the complexation between the tetrahedral component and CB[8] may also complicate the study for the supramolecular antidote. SOFs have a hydrodynamic diameter which depends on the concentration of the monomers. The size of the supramolecular polymer may impose an important influence on its efficacy as well as its toxicity. Before clinical translation, several structure-related complications and limitations have to be addressed.

MATERIALS AND METHODS

Study design

The aim of this study was to discover and develop high water-soluble porous organic polymers as the universal anticoagulant antidotes for both UFH and LMWHs. The potential of two kinds

of polycationic porous organic polymers, including SOFs and POPs, as protamine surrogates were systematically assessed. The binding affinities of SOFs and POPs with heparin were investigated with ITC and fluorescence titration experiments. The binding mechanism between the porous polymers and heparins was studied by DLS experiments. *In vitro* heparin neutralization activities were conducted in human blood samples (platelet poor plasma and whole blood) that provided by Shanghai Blood Center, using an approved protocol by Shanghai Municipal Commission of Health and Family Planning and commercial bovine platelet poor plasma. *In vivo* efficacy was studied in ICR mice or SD rats that purchased from Laboratory Animal Center of the Shanghai Institute of Planned Parenthood Research, with protocols approved by the respective Institutional Animal Care Committees of Shanghai. Six to ten animals per group with half female and male were selected to perform statistical analysis. The animals were randomized to the control and experimental groups on the basis of their body weight, but the investigator was not blind to the groups. The animals were bred in a 12 h light/dark cycle in a room with temperature and humidity controlled, grouped cages as appropriate, and allowed to have ad libitum access to sterilized tap water and standard chow. Dose tolerance and acute toxicity studies were assessed via i.v. administration of escalating doses of **SOF1** and **POP1** in ICR mice. Additional safety evaluation experiments for **SOF1**, including TEG (conducted in HWB), hemolysis assays (assessed in human and rat RBCs) and cell cytotoxicity (studied with MTT assay using the normal cardiac myoblast of rat heart cells and human breast cancer cells), were also tested. Detailed synthetic procedures and experimental protocols were included in the Supplementary Materials and Methods.

Statistical analysis

Statistical analysis of the data was carried out by one-way ANOVA test, and results are presented as either means ± SD or means ± SEM. P values of ≤ 0.05 were considered significant. The statistical test and P values are included in the figures and tables.

SUPPLEMENTARY MATERIALS

References (*52-56*).

REFERENCES AND NOTES

1. J. I. Weitz, Low-Molecular-Weight Heparins. *New Engl. J. Med.* **337**, 688-698 (1997).
2. M. Suranyi, J. S. Chow, Review: anticoagulation for haemodialysis. *Nephrology (Carlton)* **15**, 386-392 (2010).
3. A. Vincentelli, B. Jude, S. Bélisle, Antithrombotic therapy in cardiac surgery. *Can. J. Anaesth.* **53**, S89-S102 (2006).
4. S. E. Claudel, L. A. Miles, M. Murea, Anticoagulation in hemodialysis: A narrative review. *Semin. Dial.* **34**, 103-115 (2021).
5. C. W. Francis, Prophylaxis for Thromboembolism in Hospitalized Medical Patients. *New Engl. J. Med.* **356**, 1438-1444 (2007).
6. F. W. Blaisdell, Heparin-controversies and misconceptions. *J. Cardiovasc. Surg.* **4**, 691-700 (1996).
7. M. A. Crowther, T. E. Warkentin, Bleeding risk and the management of bleeding complications in patients undergoing anticoagulant therapy: focus on new anticoagulant agents. *Blood* **111**, 4871-4879 (2008).
8. M. T. Kalathottukaren, C. A. Haynes, J. N. Kizhakkedathu, Approaches to prevent bleeding associated with anticoagulants: current status and recent developments. *Drug Deliv. Transl. Res.* **8**, 928-944 (2018).
9. M. Wolzt, A. Weltermann, M. Nieszpaur-Los, B. Schneider, A. Fassolt, K. Lechner, H. G. Eichler, P. A. Kyrle, Studies on the neutralizing effects of protamine on unfractionated and low molecular weight heparin (Fragmin) at the site of activation of the coagulation system in man. *Thromb. haemost.* **73**, 439-443 (1995).
10. E. Sokolowska, B. Kalaska, J. Miklosz, A. Mogielnicki, The toxicology of heparin reversal with protamine: past, present and future. *Expert. Opin. Drug Metab. Toxicol.* **12**, 897-909 (2016).
11. B. Ourri, L. Vial, Lost in (Clinical) Translation: Recent Advances in Heparin Neutralization and Monitoring. *ACS Chem. Biol.* **14**, 2512-2526 (2019).
12. M. A. Crowther, L. R. Berry, P. T. Monagle, A. K. C. Chan, Mechanisms responsible for the failure of protamine to inactivate low-molecular-weight heparin. *Br. J. Haematol.* **116**, 178-186 (2002).
13. P. L. F. Giangrande, Fondaparinux (Arixtra): a new anticoagulant. *Int. J. Clin. Pract.* **56**, 615-617 (2002).
14. B. Brenner, R. Hoffman, Emerging options in the treatment of deep vein thrombosis and pulmonary embolism. *Blood Rev.* **25**, 215-221 (2011).
15. Y. S., M. S.R., C. S., A. R., P. J., G. C.B., A. Budaj, R. J. G. Peters, J.-P. Bassand, L. W. Joyner, K. A. A. Fox, Comparison of Fondaparinux and Enoxaparin in Acute Coronary Syndromes. *New Engl. J. Med.* **354**, 1464-1476 (2006).
16. F. Schiele, N. Meneveau, M. F. Seronde, V. Descotes-Genon, J. Dutheil, R. Chopard, F. Ecarnot, J.-P. Bassand, Routine use of fondaparinux in acute coronary syndromes: A 2-year multicenter experience. *Am. Heart J.* **159**, 190-198 (2010).
17. M. Nybo, J. S. Madsen, Serious Anaphylactic Reactions due to Protamine Sulfate: A Systematic Literature Review. *Basic Clin. Pharmacol. Toxicol.* **103**, 192-196 (2008).
18. A. Singla, M. J. Sullivan, G. Lee, J. Bartholomew, S. Kapadia, R. H. Aster, B. R. Curtis, Protamine-induced immune thrombocytopenia. *Transfusion* **53**, 2158-2163 (2013).
19. T. Bakchoul, H. Zollner, J. Amiral, S. Panzer, S. Selleng, T. Kohlmann, S. Brandt, M. Delcea, T. E. Warkentin, U. J. Sachs, A. Greinacher, Anti-protamine-heparin antibodies: incidence, clinical relevance, and pathogenesis. *Blood* **121**, 2821-2827 (2013).
20. G. M. Lee, I. J. Welsby, B. Phillips-Bute, T. L. Ortel, G. M. Arepally, High incidence of antibodies to protamine and protamine/heparin complexes in patients undergoing cardiopulmonary bypass. *Blood* **121**, 2828-2835 (2013).
21. J. J. van Veen, R. M. Maclean, K. K. Hampton, S. Laidlaw, S. Kitchen, P. Toth, M. Makris, Protamine reversal of low molecular weight heparin: clinically effective? *Blood Coagul. Fibrin.* **22**, 565-570 (2011).
22. S. M. Bromfield, E. Wilde, D. K. Smith, Heparin sensing and binding - taking supramolecular chemistry towards clinical applications. *Chem. Soc. Rev.* **42**, 9184-9195 (2013).
23. D. Marson, E. Laurini, S. Aulic, M. Fermeglia, S. Pricl, Unchain My Blood: Lessons Learned from Self-Assembled Dendrimers as Nanoscale Heparin Binders. *Biomolecules* **9**, 385 (2019).
24. H. Yin, X. Zhang, J. Wei, S. Lu, D. Bardelang, R. Wang, Recent advances in supramolecular antidotes. *Theranostics* **11**, 1513-1526 (2021).

25. S. Choi, D. J. Clements, V. Pophristic, I. Ivanov, S. Vemparala, J. S. Bennett, M. L. Klein, J. D. Winkler, W. F. DeGrado, The design and evaluation of heparin-binding foldamers. *Angew. Chem. Int. Ed.* **44**, 6685-6689 (2005).
26. A. C. Rodrigo, A. Barnard, J. Cooper, D. K. Smith, Self-assembling ligands for multivalent nanoscale heparin binding. *Angew. Chem. Int. Ed.* **50**, 4675-4679 (2011).
27. J. E. Ansell, B. E. Laulicht, S. H. Bakhru, M. Hoffman, S. S. Steiner, J. C. Costin, Ciraparantag safely and completely reverses the anticoagulant effects of low molecular weight heparin. *Thromb. Res.* **146**, 113-118 (2016).
28. P. Y. Li, Y. Chen, C. H. Chen, Y. Liu, Amphiphilic multi-charged cyclodextrins and vitamin K co-assembly as a synergistic coagulant. *Chem. Commun.* **55**, 11790-11793 (2019).
29. Q. Huang, H. Zhao, M. Shui, D. S. Guo, R. Wang, Heparin reversal by an oligoethylene glycol functionalized guanidinocalixarene. *Chem. Sci.* **11**, 9623-9629 (2020).
30. R. A. Shenoi, M. T. Kalathottukaren, R. J. Travers, B. F. L. Lai, A. L. Creagh, D. Lange, K. Yu, M. Weinhart, B. H. Chew, C. Du, D. E. Brooks, C. J. Carter, J. H. Morrissey, C. A. Haynes, J. N. Kizhakkedathu, Affinity-based design of a synthetic universal reversal agent for heparin anticoagulants. *Sci. Transl. Med.* **6**, 260ra150 (2014).
31. S. Valimaki, A. Khakalo, A. Ora, L. S. Johansson, O. J. Rojas, M. A. Kostiainen, Effect of PEG-PDMAEMA Block Copolymer Architecture on Polyelectrolyte Complex Formation with Heparin. *Biomacromolecules* **17**, 2891-2900 (2016).
32. J. Wen, M. Weinhart, B. Lai, J. Kizhakkedathu, D. E. Brooks, Reversible hemostatic properties of sulfabetaine/ quaternary ammonium modified hyperbranched polyglycerol. *Biomaterials* **86**, 42-55 (2016).
33. B. Ourri, J. P. Francoia, G. Monard, J. C. Gris, J. Leclaire, L. Vial, Dendrigraft of Poly-l-lysine as a Promising Candidate To Reverse Heparin-based Anticoagulants in Clinical Settings. *ACS Med. Chem. Lett.* **10**, 917-922 (2019).
34. E. P. Bianchini, A. Sebestyen, T. Abache, Y. Bourti, A. Fontayne, V. Richard, F. Tamion, J.-L. Plantier, F. Doguet, D. Borgel, Inactivated antithombin as anticoagulant reversal in a rat model of cardiopulmonary bypass: a potent and potentially safer alternative to protamine. *Br. J. Haematol.* **180**, 715-720 (2018).
35. S. Välimäki, Q. Liu, L. Schoonen, D. F. M. Vervoort, Nonappa, V. Linko, R. J. M. Nolte, J. C. M. van Hest, M. A. Kostiainen, Engineered protein cages for selective heparin encapsulation. *J. Mat. Chem. B* **9**, 1272-1276 (2021).
36. V. Forster, J.-C. Leroux, Nano-antidotes for drug overdose and poisoning. *Sci. Trans. Med.* **7**, 290ps214-290ps214 (2015).
37. C. L. Deng, S. L. Murkli, L. D. Isaacs, Supramolecular hosts as in vivo sequestration agents for pharmaceuticals and toxins. *Chem. Soc. Rev.* **49**, 7516-7532 (2020).
38. H. Yin, D. Bardelang, R. Wang, Macrocycles and Related Hosts as Supramolecular Antidotes. *Trends Chem.* **3**, 1-4 (2021).
39. M. T. Kalathottukaren, A. L. Creagh, S. Abbina, G. Lu, M. J. Karbarz, A. Pandey, P. B. Conley, J. N. Kizhakkedathu, C. Haynes, Comparison of reversal activity and mechanism of action of UHRA, andexanet, and PER977 on heparin and oral FXa inhibitors. *Blood Adv.* **2**, 2104-2114 (2018).
40. F. F. Becker Studies on the Hemolytic Properties of Protamine. *J. Gen. Physiol.* **44**, 433-442 (1961).
41. J. Tian, T. Y. Zhou, S. C. Zhang, S. Aloni, M. V. Altoe, S. H. Xie, H. Wang, D. W. Zhang, X. Zhao, Y. Liu, Z. T. Li, Three-dimensional periodic supramolecular organic framework ion sponge in water and microcrystals. *Nat. Commun.* **5**, 5574 (2014).
42. J. Tian, H. Wang, D.-W. Zhang, Y. Liu, Z.-T. Li, Supramolecular organic frameworks (SOFs): homogeneous regular 2D and 3D pores in water. *Nat. Sci. Rev.* **4**, 426-436 (2017).
43. B. Yang, X.-D. Zhang, J. Li, J. Tian, Y.-P. Wu, F.-X. Yu, R. Wang, H. Wang, D.-W. Zhang, Y. Liu, L. Zhou, Z.-T. Li, In Situ Loading and Delivery of Short Single- and Double-Stranded DNA by Supramolecular Organic Frameworks. *CCS Chem.* **1**, 156-165 (2019).
44. Z. Z. Gao, Z. K. Wang, L. Wei, G. Yin, J. Tian, C. Z. Liu, H. Wang, D. W. Zhang, Y. B. Zhang, X. Li, Y. Liu, Z. T. Li, Water-Soluble 3D Covalent Organic Framework that Displays an Enhanced Enrichment Effect of Photosensitizers and Catalysts for the Reduction of Protons to H2. *ACS Appl. Mater. Interfaces* **12**, 1404-1411 (2020).

45. F. Biedermann, W. M. Nau, H.-J. Schneider, The Hydrophobic Effect Revisited—Studies with Supramolecular Complexes Imply High-Energy Water as a Noncovalent Driving Force. *Angew. Chem. Int. Ed.* **53**, 11158-11171 (2014).
46. J. Harenberg, Is laboratory monitoring of low-molecular-weight heparin therapy necessary? Yes. *J. Thromb. Haemost.* **2**, 547-550 (2004).
47. E. Gray, B. Mulloy, T. W. Barrowcliffe, Heparin and low-molecular-weight heparin. *Thromb. Haemost.* **99**, 807-818 (2008).
48. D. Bolliger, M. D. Seeberger, K. A. Tanaka, Principles and Practice of Thromboelastography in Clinical Coagulation Management and Transfusion Practice. *Transfus. Med. Rev.* **26**, 1-13 (2012).
49. G. Lu, F. R. DeGuzman, S. J. Hollenbach, M. J. Karbarz, K. Abe, G. Lee, P. Luan, A. Hutchaleelaha, M. Inagaki, P. B. Conley, D. R. Phillips, U. Sinha, A specific antidote for reversal of anticoagulation by direct and indirect inhibitors of coagulation factor Xa. *Nat. Med.* **19**, 446-451 (2013).
50. V. D. Uzunova, C. Cullinane, K. Brix, W. M. Nau, A. I. Day, Toxicity of cucurbit[7]uril and cucurbit[8]uril: an exploratory in vitro and in vivo study. *Org. Biomol. Chem.* **8**, 2037-2042 (2010).
51. F. Li, A. K. Gorle, M. Ranson, K. L. Vine, R. Kinobe, M. Feterl, J. M. Warner, F. R. Keene, J. G. Collins, A. I. Day, Probing the pharmacokinetics of cucurbit[7, 8 and 10]uril: and a dinuclear ruthenium antimicrobial complex encapsulated in cucurbit[10]uril. *Org. Biomol. Chem.* **15**, 4172-4179 (2017).
52. V. Diemer, H. Chaumeil, A. Defoin, P. Jacques, C. Carré, Synthesis of 4-[N-methyl-4-pyridinio]-phenolate (POMP) and negative solvatochromism of this model molecule in view of nonlinear optical applications. *Tetrahedron Lett.* **46**, 4737-4740 (2005).
53. J. Tian, Y. D. Ding, T. Y. Zhou, K. D. Zhang, X. Zhao, H. Wang, D. W. Zhang, Y. Liu, Z. T. Li, Self-assembly of three-dimensional supramolecular polymers through cooperative tetrathiafulvalene radical cation dimerization. *Chem. Eur. J.* **20**, 575-584 (2014).
54. Y. Zhang, J. Wang, P. Jia, X. Yu, H. Liu, X. Liu, N. Zhao, B. Huang, Two-photon fluorescence imaging of DNA in living plant turbid tissue with carbazole dicationic salt. *Org. Biomol. Chem.* **8**, 4582-4588 (2010).
55. J. Thomas, T. Cash Michael. (BECTON, DICKINSON AND COMPANY, 2008).
56. R. Krieg, A. Eitner, W. H. H. Günther, K. J. Halbhuber, Optimization of heterocyclic 4-hydroxystyryl derivatives for histological localization of endogenous and immunobound peroxidase activity. *Biotech. Histochem.* **82**, 235 - 262 (2007).

Acknowledgments: We thank Shanghai Blood Center for providing human platelet poor plasma and human whole blood for scientific research. SAXS data were collected with beamline BL16B1 at Shanghai Synchrotron Radiation Facility as well as SIBYLS beamline 12.3.1 and 7.3.3 at the Advanced Light Source (ALS), which are greatly appreciated. SAXS data collection at SIBYLS is funded through DOE BER Integrated Diffraction Analysis Technologies (IDAT) program and NIGMS grant P30 GM124169-01, ALS-ENABLE.

Funding: Z.T.L. thanks financial supports from the National Natural Science Foundation of China (Nos. 21890732, 21890730 and 21921003). F.L. thanks Chinese Postdoctoral Science Foundation (2021M693278) and Shanghai "Super Postdoc" Incentive Plan for financial supports.

Author contributions: F.L., S.B.Y., Y.Y.L, C.Z.L, S.L., J.C., Q.Y.Q., Y.L. and J.T. performed experiments. F.L., S.B.Y., W.Z. and Z.T.L. designed experiments and analyzed data. X.L., Y.L. and J.T. analyzed the data. F.L. and S.B.Y., W.Z. and Z.T.L. wrote the manuscript. Z.T.L. conceived and supervised the study.

Competing interests: Z.T.L., F.L, S.B.Y., J.C., Q.Y.Q. and J.T. are listed as inventors on a patent application on the use of SOFs and POPs for heparin reversal. The other authors declare that they have no competing interests.

Data and materials availability: All data associated with this study are present in the paper or the Supplementary Materials. Proprietary reagents used during these studies are available upon request from the corresponding author.